One-handed Knotting of a Linear Flexible Object based on Reconfigurable Skill Synthesis Strategy

Yuji Yamakawa [1], Akio Namiki [2], Masatoshi Ishikawa [1], Makoto Shimojo [3]

[1] Dept. of Information Physics and Computing, University of Tokyo
Hongo 7-3-1, Bunkyo-ku, Tokyo 113-8656, Japan
Yuji_Yamakawa@ipc.i.u-tokyo.ac.jp
Masatoshi_Ishikawa@ipc.i.u-tokyo.ac.jp

[2] Dept. of Electronics and Mechanical Engineering, Chiba University
Yayoi-cho 1-33, Inage-ku, Chiba 263-8522, Japan
namiki@faculty.chiba-u.jp

[3] Dept. of Mechanical Engineering and Intelligent Systems, University of Electro-Communications
Chofugaoka 1-5-1, Chofu-shi, Tokyo 182-8585, Japan
shimojo@mce.uec.ac.jp

Abstract—*This paper illustrates the relationship between a knotting process and knotting skills for a multifingered hand. To determine the appropriate skills required for knotting, we analyzed the knotting motion performed by a human hand. The knotting process is divided into four handling skills. In addition, this paper proposes a new strategy for making knots with a multifingered hand. The strategy consists of several basic skills, and various knots can be achieved by reconfigurable synthesis of skills. Finally, we show experimental results of an overhand knot and a half hitch.*

Index Terms—*Reconfigurable Mechanisms, Reconfigurable Robots*

1. Introduction

Manipulation of linear flexible objects is an important topic in robotics research. Recently, there has been an increasing need for automated manipulation of linear flexible objects in several applications, for example, wiring of electrical cables, stitching in surgery, and so on. The objective of this study is to manipulate a linear flexible object dexterously. As an example, we consider knotting of a flexible rope.

First, we extract several basic skills for knotting based on an original knot theory, and we explain a reconfigurable knotting strategy in which several knots are achieved by synthesizing these skills, as shown in Fig. 1(a). Each skill is related to an actual motion of a multifingered hand.

Second, we propose a trajectory planning and control method for each skill. In the method, visual and tactile feedback controls are used.

Lastly, two kinds of knot (overhand knot and half hitch) were realized using a high-speed multifingered hand system.

2. Related Works

Several researchers have focused on manipulation of linear flexible objects. For example, Inaba et al. proposed a method of knotting a rope with a manipulator [1]. Matsuno et al. used an imaging system to recognize the shape of a rope and demonstrated knotting using dual manipulators [2]. Morita et al. proposed a knot planning technique using a system called Knot Planning from Observation (KPO) [3]. Wakamatsu et al. formulated a description of knots and a process of knot manipulation [4]. That study considered the geometry of the knot and proposed a knotting process.

However, in the above studies, the analysis of knot geometry is the main topic. In their experiments, a manipulator was controlled along a trajectory based on the knot geometry. However, the characteristics of the manipulator and end-effector were not considered. As a result, the motion of the

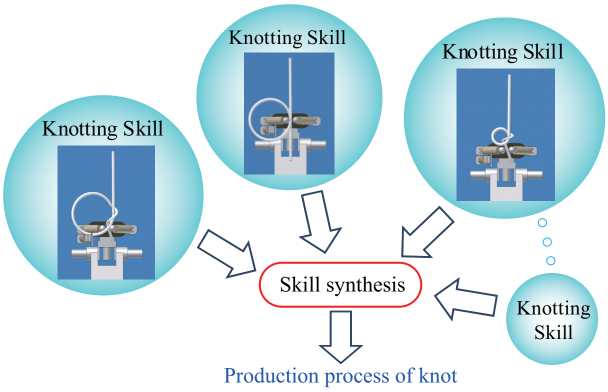

(a) Skill synthesis.

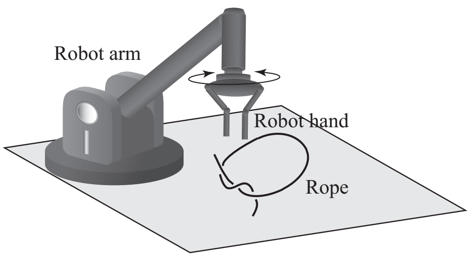

(b) Concept.

Fig. 1. Knotting of a flexible rope.

manipulator become redundant. In order to achieve knotting at high-speed, it is necessary to develop the skills required by a manipulator and an end-effector for knotting. The aim of this research is to identify the manipulation skills required by a general robot arm and robot hand to achieve a knotting task, as shown in Fig. 1(b).

3. Production Process of Knots

This section explains the method used to obtain the production process of a knot in order to achieve the knotting task by a robot system. In this paper, "task" is defined as one manipulation achieved by the robot, and "skill" is defined as a minimum required element to achieve the task and a significant element that changes the rope state. Therefore, one "task" is achieved by the combination of some "skills".

3.1. Extraction of Knotting Skills

There are two main difficulties in manipulating a flexible linear object:

1) Controlling the deformation of the rope during manipulation, and
2) Predicting the rope deformation.

To overcome these difficulties, the following strategies are considered:

1) Using sensory feedback control by real-time measurement of the rope deformation, and
2) Developing manipulation skills that do not depend on the flexible characteristics of a rope.

In this paper, we focus on developing a manipulation skill that does not depend on the flexible characteristics of the rope and sensory feedback control.

In order to identify manipulation skills required for knotting, we analyzed a one-handed knotting process performed by a human hand, as shown in Fig. 2. Fig. 2(a) is the initial state, Fig. 2(b) shows loop production by arm motion, Fig. 2(c) shows rope permutation by finger motion, and Fig. 2(d) shows rope pulling by arm motion. As a result, we identified three skills required to achieve one-handed knotting: loop production, rope permutation, and rope pulling.

In addition, in order to allow handling of the ends of the rope, one more manipulation skill called rope moving is added. In summary, the essential manipulation skills for knotting are: **1) Loop production, 2) Rope permutation, 3) Rope pulling, and 4) Rope moving**.

The production process of a knot can be obtained by the combination of the above skills, as explained below. Therefore, the identified skills are reconfigurable ones.

3.2. Description of Knot

We define the description of a rope intersection that constitutes the knot by referring to the method proposed in [4].

The beginning of a rope is represented by E_l as the initial location. In the same way, the end of the rope is represented by E_r as the final location. Descriptions of the intersections $C_i^{\{+,-\}}(i = 1, 2, 3\cdots)$ are assigned for all intersections from E_l to E_r, where i is an intersection number. The sign "$+, -$"

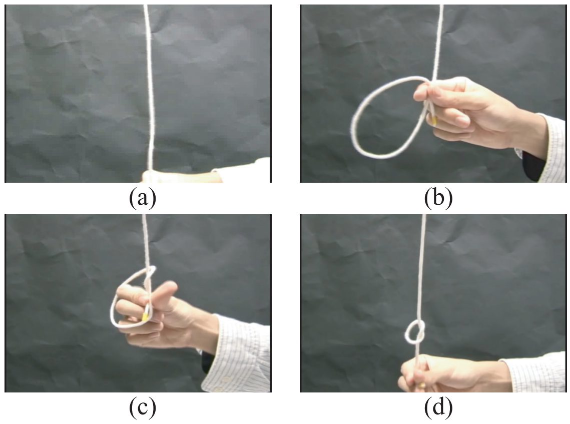

Fig. 2. One-handed knotting by human hand.

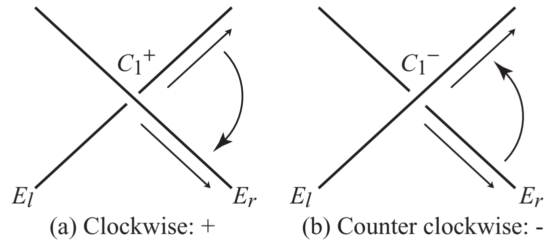

Fig. 3. Intersection sign [4].

shows the intersection sign. The sign is defined as follows: First, we focus on the two directions of the rope at the "outlet" of the intersection. Second, the lower rope is rotated clockwise or counterclockwise so as to match the two directions of the rope. If the lower rope is rotated clockwise, the sign is defined as "+", as shown in Fig. 3(a). If the lower rope is rotated counterclockwise, the sign is defined as "−", as shown in Fig. 3(b). As a result, the description of the intersection is defined as shown in Fig. 3.

Moreover, we introduce a new description here. First, the two directions of the rope at the "outlet" of the intersection are summed. Second, the line that connects the two fingers grasping the intersection is considered. Last, the relationship between the summed rope direction and this connecting line is examined. If the relationship is parallel, the description of the intersection is defined as $\overline{C_1^+}$, as shown in Fig. 4(a). If the relationship is orthogonal, the description of the intersection is defined as $\widehat{C_1^+}$, as shown in Fig. 4(b). This description method is used in loop production, in particular.

The characteristics and the description of each skill have been examined based on the proposed description method [5].

3.3. Skill Synthesis

In this section, we analyze the feasibility of some knots based on skill synthesisand then propose a knot production process.

Analysis Method

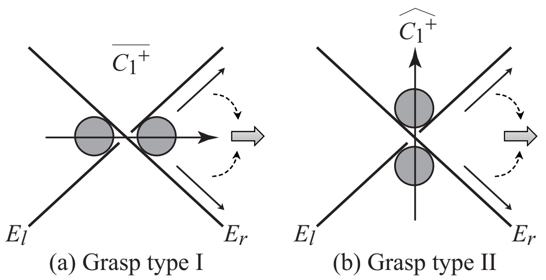

Fig. 4. Grasp type.

1) Represent a knot based on the description of the intersections that constitute the knot.
2) Unravel one intersection of the knot, starting from the intersection nearest the end of the rope.
3) Iterate 2) until the intersections disappear. As a result, a sequence of operations to remove the intersections is obtained.
4) Apply appropriate skills to the sequence, while following the sequence obtained in 3) in reverse.

By this process, the location and sign of each intersection is identified. As a result, it can be determined how to generate the intersections. This analysis can be applied not only to a knot generated by one rope, but also to a knot generated by one rope and one object and to a knot generated by two ropes. Although the knot production process obtained by the proposed analysis method may not be optimal, this method can always provide one solution for the knot production process.

3.3.1) Knot Generated by One Rope: As an example, here we analyze an "overhand knot" (Fig. 5(a)). An overhand knot is the simplest knot that is created on a rope. This knot prevents the rope unraveling.

Analysis of overhand knot

First, the description of the intersection in the overhand knot is

$$E_l - C_1^- - C_2^- - C_3^- - C_1^- - C_2^- - C_3^- - E_r. \text{ (Fig. 5(a))}$$

Next, removing one intersection (C_3^-), starting from the intersection near the end (E_r) of the rope, gives the following description of the intersections of the overhand knot:

$$E_l - C_1^- - C_2^- - C_1^- - C_2^- - E_r \text{ (Fig. 5(b))}$$

Iterating this operation until the intersections disappear yields the following description of the intersection

$$E_l - C_1^- - C_1^- - E_r \text{ (Fig. 5(c))}$$
$$E_l - E_r \text{ (Fig. 5(d))}.$$

The production process of the overhand knot can be obtained by following this process in reverse while considering the description of the intersections.

Production process of overhand knot

First, loop production is performed, and the intersection $\widehat{C_1^-}$ is created (Fig. 6(a)). Second, the intersection C_2^- is produced. However, it is not effective to produce only the

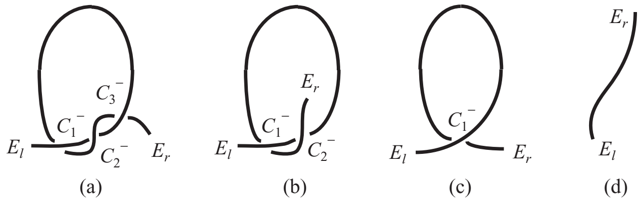

Fig. 5. Analysis of overhand knot.

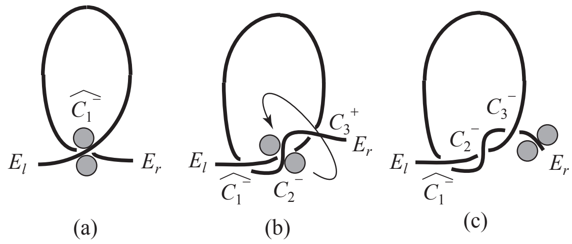

Fig. 6. Production process of overhand knot.

intersection C_2^-. By checking the final type of knot, it is found that two intersections should be made after the intersection $\widehat{C_1^-}$. In addition, the final intersection C_3^- should pass under the rope. For these reasons, the state shown in Fig. 6(b) can be produced only by performing rope permutation. Last, using rope permutation and rope pulling, the overhand knot is achieved, as shown in Fig. 6(c). The description of the intersections for the overhand knot production process can be represented by the following:

$$E_l - E_r \text{ (Fig. 5(d))}$$
$$E_l - \widehat{C_1^-} - \widehat{C_1^-} - E_r \text{ (Fig. 6(a))}$$
$$E_l - \widehat{C_1^-} - C_2^- - C_3^+ - \widehat{C_1^-} - C_2^- - C_3^+ - E_r \text{ (Fig. 6(b))}$$
$$E_l - \widehat{C_1^-} - C_2^- - C_3^- - \widehat{C_1^-} - C_2^- - C_3^- - E_r \text{ (Fig. 6(c))}$$

The eight knot and the stevedore's knot can be produced based on skill synthesis in the same way.

3.3.2) Knot Generated by One Rope and One Object: In this section, we consider the knotting process of a knot generated by one rope and one object. As an example, we analyze a "half hitch" (Fig. 7). The half hitch is one of the knots that make a connection between a rope and an object.

Production process of half hitch

Here, we omit the intersection description of the half hitch. The left end and the right end of the rope are represented by l_1 and l_2, and the left end and the right end of the object are represented by r_1 and r_2. The description of intersections on the rope and the object is performed in the order of initial location.

First, the intersection C_1^+ is created by rope permutation (Fig. 7(b), (c)). Second, the rope is wrapped around the stick by rope moving to produce the intersection C_2^+ (Fig. 7(d)). Next, the intersection $\widehat{C_1^-}$ is made by loop production (Fig. 7(e)). Lastly, the half hitch is finished by performing rope permutation twice and rope pulling once (Fig. 7(f), (g)).

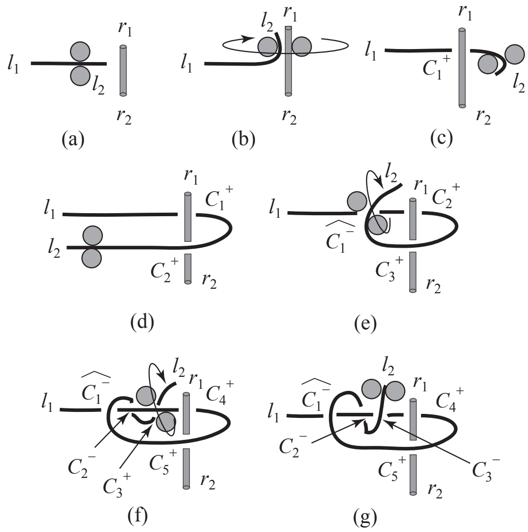

Fig. 7. Production process of half hitch.

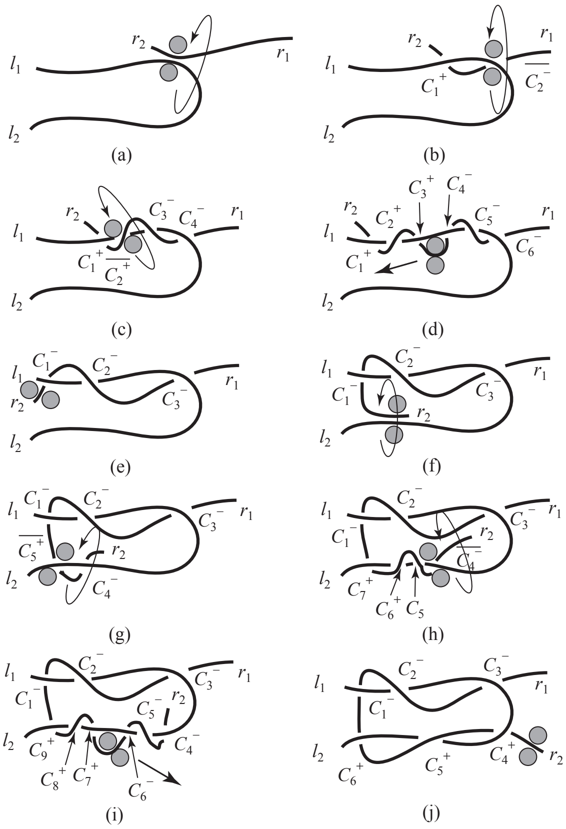

Fig. 8. Production process of square knot.

3.3.3) Knot Generated by Two Ropes: In this section, the production process of a knot generated by two ropes is explained. As an example, the "square knot" (Fig. 8) is analyzed. The description of the intersection is the same as that for the knot generated by one rope and one object.

Production process of square knot

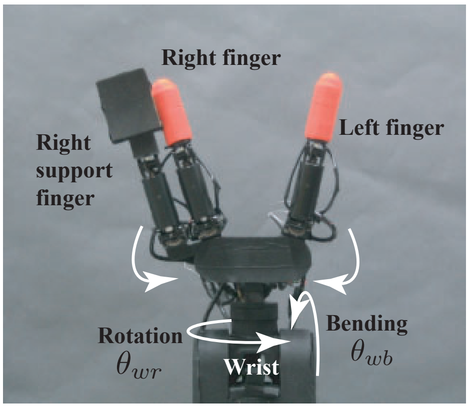

Fig. 9. Photograph of robot hand.

(a) Tactile sensor

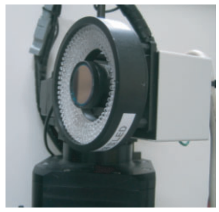

(b) Vision sensor

Fig. 10. Photographs of tactile and vision sensors.

First, the two ropes are set as shown in Fig. 8(a). Second, the intersections (C_1^-, C_2^- and C_3^-) are produced by three rope permutations and rope pulling, as shown in Fig. 8(b) $\sim$ (e). Third, the two ropes are set as shown in Fig. 8(f) by rope moving. Lastly, the intersections (C_4^+, C_5^+ and C_6^+) are produced by three rope permutations and rope pulling, as shown in Fig. 8(g)–(j).

As a result, the production process of a knot can be obtained by skill synthesis. Namely, it is considered that the extracted skills are reconfigurable ones.

4. High-speed Multifingered Hand System

Fig. 9 shows the mechanical design of the hand [6]. As shown in Fig. 9, the hand has three fingers: a left finger, a right finger, and a right support finger. Moreover, the hand has two wrist joints. The joints of the hand can be closed at a speed of 180 deg./0.1 s. In order to prevent the rope from slipping on the fingers of the robot hand, a fingerstall is attached to each top link, as shown in Fig. 9.

Fig. 10(a) shows one of the high-speed tactile sensors [7]. This sensor is a sheet-like object, and its weight is only $0.2\,\mathrm{g/cm^2}$. The center position of a two-dimensional distributed load and the total load are measured within 1 ms by this sensor. A tactile sheet is attached to the top link of each finger.

Fig. 10(b) shows the high-speed visual sensor (Column Parallel Vision II, simply called CPV-II) [8]. The CPV-II has 128×128 photo-detectors, an all pixel parallel processing array based on the vision chip architecture, and an exclusive

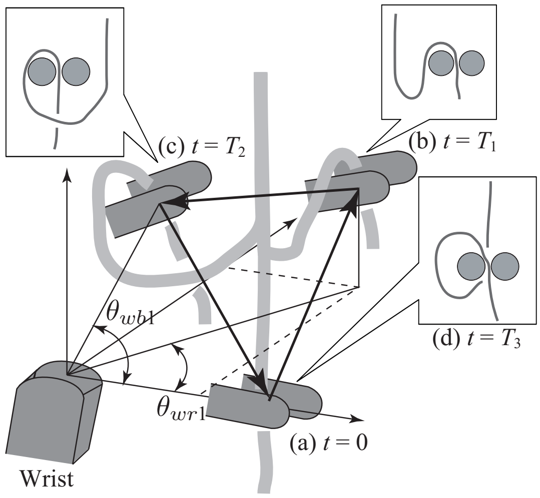

Fig. 11. Loop production.

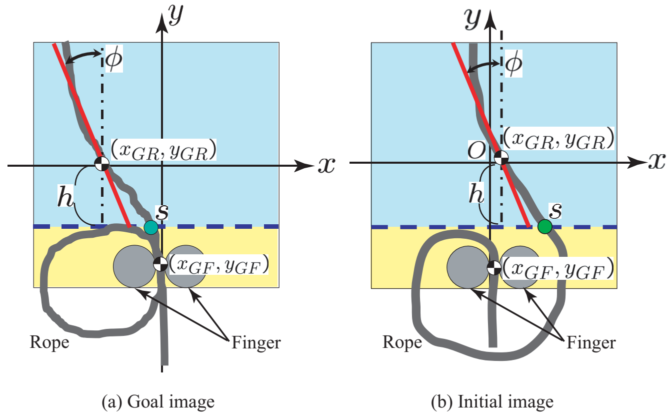

Fig. 12. Image of high-speed vision system.

summation circuit for calculating moment values. Since visual processing is executed in parallel in the processing array, high-speed visual processing (moment detection and segmentation) can be achieved within 1 ms.

CPV-II is mounted on an Active Vision system that has pan and tilt mechanisms. The Active Vision system can track a target within 1 ms.

5. Knotting Strategy

In this section, new strategies for knotting skills are suggested. Each strategy is achieved so as not to depend on the flexible characteristics of a rope. That is to say, the proposed strategy itself is robustness against rope deformation. Since the strategy of rope moving is executed by the robot arm, this paper does not explain that strategy.

5.1. Loop production

5.1.1) Trajectory of the wrist: In this skill, a loop that serves as the starting point of the knot is produced on the rope. First, the rope is grasped by two fingers. A loop is produced by rotation and bending of the two wrist joints so as to twist the rope around the finger (Fig. 11). The reference trajectory of the wrist joint angle is given as follows:

$$\theta_{wb} = \theta_{wb1}\frac{t}{T_1}, \quad \theta_{wr} = \theta_{wr1}\frac{t}{T_1} \quad (0 \le t \le T_1) \tag{1}$$

$$\theta_{wb} = \theta_{wb1}, \quad \theta_{wr} = \theta_{wr1}\left(\frac{T_2 - t}{T_2 - T_1}\right) \quad (T_1 < t \le T_2) \tag{2}$$

$$\theta_{wb} = \theta_{wb1}\left(\frac{T_3 - t}{T_3 - T_2}\right), \quad \theta_{wr} = 0 \quad (T_2 < t \le T_3), \tag{3}$$

where θ_{wr} and θ_{wb} are the rotation and bending reference joint angles of the wrist, θ_{wr1} and θ_{wb1} are the maximum rotation and bending joint angles of the wrist, t is time, and T_1, T_2, and T_3 are the transition times from Fig. 11(a) to (b), from (b) to (c), and from (c) to (d), respectively.

5.1.2) Visual feedback control: In Fig. 11(c)–(d), there exists a case where the other rope cannot be grasped by the hand. Thus, in order to improve the success rate of loop production, visual feedback control is introduced.

First, the image taken by the CPV-II is divided into two regions. One region is used for tracking the finger. The other region is used for calculating the state of the rope.

Fig. 12(b) shows the image obtained by the CPV-II during loop production. In the lower region (Fig. 12, yellow region), the image center of the two fingers (x_{GF}, y_{GF}) is calculated. Then, based on this value, finger tracking is performed. In the upper region (Fig. 12, blue region), the image center (x_{GR}, y_{GR}) and the angle ϕ of the principal axes of the rope are calculated. The wrist joint angle of the robot hand is controlled from these three pieces of information about the rope.

Second, the x coordinate of the rope at the boundary of the image is estimated. Assuming that the angle ϕ of the principal axes of the rope is very small, the following equation can be obtained:

$$x_s = x_{GR} + h \tan\phi \approx x_{GR} + h\phi \tag{4}$$

where h is the distance between the boundary (dash line) and the y center position, y_{GR}, of the rope.

Using the relationship between the finger coordinate x_{GF} and the rope coordinate x_s, the rotation reference joint angle of the wrist in Eqn. (3) is modified by the following equation:

$$\theta_{wr} = k(x_s - x_{GF}) \tag{5}$$

where k is an appropriate feedback gain. Namely, the wrist joint is controlled so as to conform the finger coordinate x_{GF} to the rope coordinate x_s. The proposed visual feedback control is used in Fig. 11(c)–(d).

Fig. 13 shows the experimental result obtained with the proposed visual feedback control method for loop production. Fig. 14 shows the x coordinate x_s of the rope on the boundary and the image center of the finger x_{FG}, respectively. Fig. 13(a) to Fig. 13(e) show the action where the rope is twisted on the finger. Fig. 13(e) to Fig. 13(i) show the grasping motion. In the

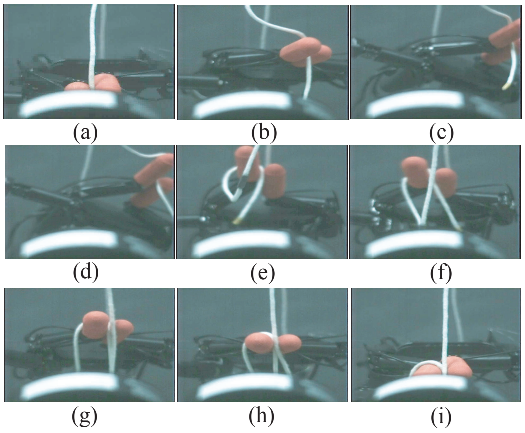

Fig. 13. Continuous photographs of loop production controlled by visual feedback.

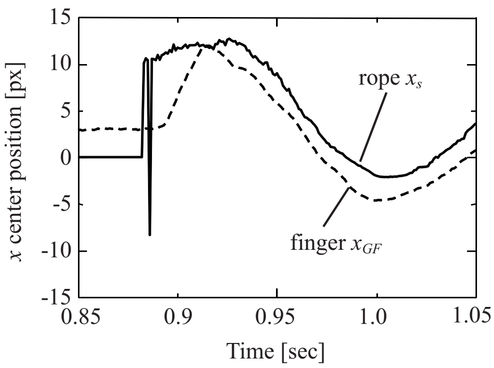

Fig. 14. Experimental result of visual feedbacks

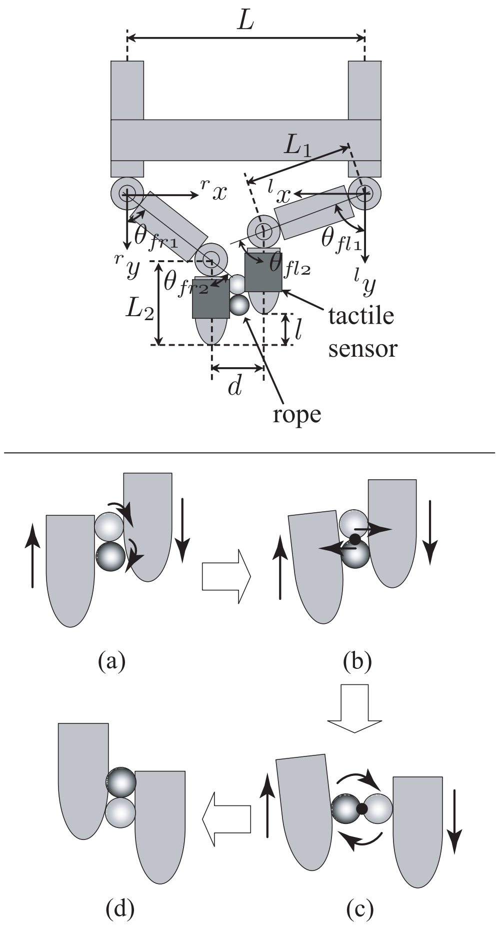

Fig. 15. Strategy of rope permutation.

grasping motion, the proposed visual feedback control method is performed.

It can be seen from Fig. 14 that the wrist joint angle of the robot hand is controlled so that the image center of the finger tracks the image center of the rope within 0.88–1.05 s. However, since the wrist joint angle is controlled simply by proportional control, a steady-state velocity error appears.

5.2. Rope permutation

5.2.1) Trajectory of the fingers: In order to make a knot, it is necessary to pass one end of the rope through the loop. However, it is difficult to achieve this task with one hand. As an equivalent task, permutation of two ropes is executed by rubbing two fingers together while keeping them parallel. Preparation for making a knot is completed if the ropes are permuted two times.

A strategy for rope permutation is shown in Fig. 15. The upper part in Fig. 15 shows the overall rope permutation. The lower part shows the finger motion. Both fingers are moved while remaining parallel. At some point, the two ropes engage each other by virtue of friction, as shown in Fig. 15(b). By continuing to move the two fingers in parallel, the two ropes are permuted (exchange places), as shown in Fig. 15(c) and (d).

The motion of both fingers is described by the following equation:

$$\theta_{fl1} = \theta_{fl10}\frac{T-t}{T} + \theta_{fr10}\frac{t}{T} \tag{6}$$

$$\theta_{fr1} = \sin^{-1}\left(\frac{L - L_1\sin(\theta_{fl1}) - d}{L_1}\right) \tag{7}$$

$$\theta_{fl2} = -\theta_{fl1}, \quad \theta_{fr2} = -\theta_{fr1}, \tag{8}$$

where $\theta_{fl\{1,2\}}$ are the reference joint angles of the root and tip links of the left finger, $\theta_{fr\{1,2\}}$ are the reference joint angles of the root and tip links of the right finger, θ_{fl10} and θ_{fr10} are the initial joint angles of the left and right fingers, respectively, d is the distance between both fingers, and l is the parallel movement distance. Giving the values d and l, the initial joint angles can be obtained by solving the inverse kinematics. Here, L, L_1, and L_2 are the link parameters as shown in Fig. 15, t is time, and T is the period of the rope permutation motion. The left finger motion is given by a function of time and transits from the initial joint angle of the left finger to the initial joint angle of the right finger. According to the left finger motion, the joint angle of the right finger is obtained by solving the inverse kinematics.

Moreover, the joint angle of the right finger is modified by

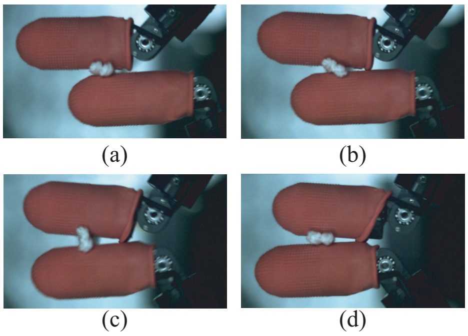

Fig. 16. Experimental result of rope permutation.

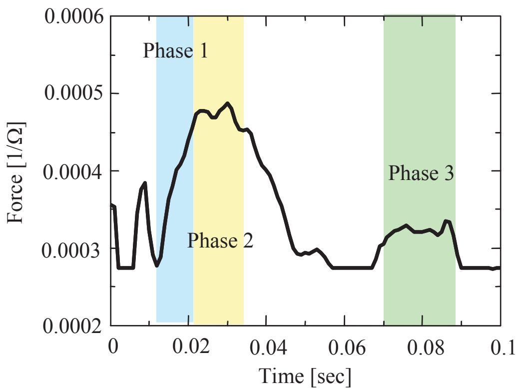

Fig. 17. Experimental result of reaction force with control.

force feedback control:

$$\theta'_{fr1} = \theta_{fr1} + J\left(k_{pf}e + k_{if}\int edt\right), \quad (9)$$

where θ'_{fr1} is the modified joint angle of the right finger, $e = f_r - F_s$, f_r is the force setpoint, F_s is the force observed by the tactile sensor, k_{pf} and k_{if} are appropriate gains, and J is the Jacobian.

5.2.2) Tactile feedback control based on estimation of phase transition: Performing the finger parallel motion, the condition of the rope permutation can be divided into three phases.

Phase 1 shows the condition where the two ropes independently rotate and do not engage (Fig. 15(a)). Phase 2 shows the condition where the two ropes engage and do not rotate (Fig. 15(b)). Phase 3 shows the condition where the two ropes permute (Fig. 15(c)). The details of rope permutation have been explained in [9]. In phase 3, the distance between both fingers is extremely important in executing the rope permutation.

Thus, a suggested control method is to use the tactile information, as follows:

1) Estimate the phase transitions. In particular, the transition to Phase 3 that needs the force control is estimated when the reaction force F_s becomes very small.
2) Increase the two gains (k_{pf},k_{if}) of the force control in Eqn. (9).

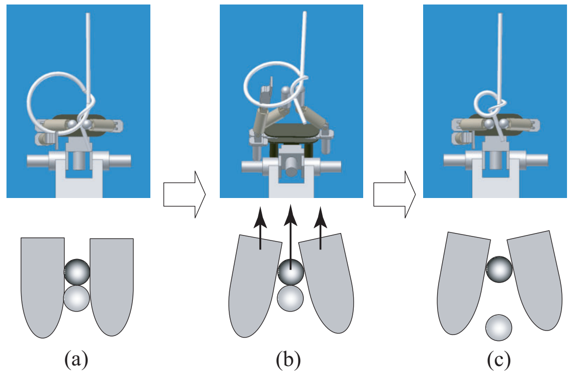

Fig. 18. Rope pulling.

Fig. 16 and Fig. 17 show continuous photographs and experimental results of force data obtained by the tactile sensor with the proposed grasping force control, respectively. From Fig. 16, the rope permutation can be carried out by the finger parallel motion and the proposed grasping force control. As can be seen from Fig. 17, the joint angle is controlled so that the grasping force will be constant. That is, the distance between both fingers can be appropriately controlled by using the grasping force control.

5.3. Rope pulling

Knotting is achieved when one of the two permuted ropes is pulled. Generally, in order to pull a rope, it is necessary to translate the robot hand vertically. Since our experimental system is not capable of parallel motion, bending and extension of the wrist joint are used instead. The rope pulling task is achieved by high-speed bending and extension motions of the wrist joint, as shown in Fig. 18.

6. Experiment

Fig. 20 and Fig 22 show sequences of continuous photographs of the knotting tasks (overhand knot and half hitch).

<u>Overhand knot</u>

The experimental system is shown in Fig. 19. Fig. 20(a)–(e) show loop production. In Fig. 20(f), the rope sections are pressed by the free finger to strengthen the contact state between the two sections. Fig. 20(g)–(i) show rope permutation. Fig. 20(j)–(l) show rope pulling.

<u>Half hitch</u>

The experimental system is shown in Fig. 21. In the initial state, the rope is wrapped around the object, as shown in Fig. 21. Fig. 22(a)–(c) show loop production. In Fig. 22(d), the rope sections are pressed by the free finger to strengthen the contact state between the two sections. Fig. 22(e)–(g) show rope permutation. Fig. 22(h) and (i) show rope pulling. Last, Fig. 22(j)–(l) show additional rope pulling by a human hand to tighten up the knot.

These video sequences can be viewed on our web site [10].

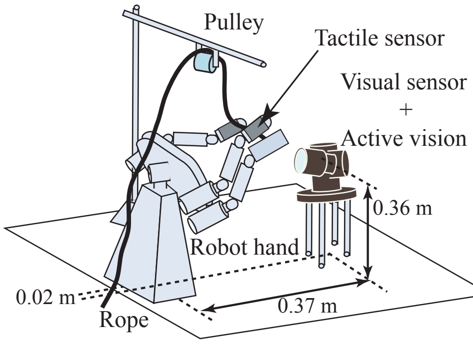

Fig. 19. Overall system for overhand knot production.

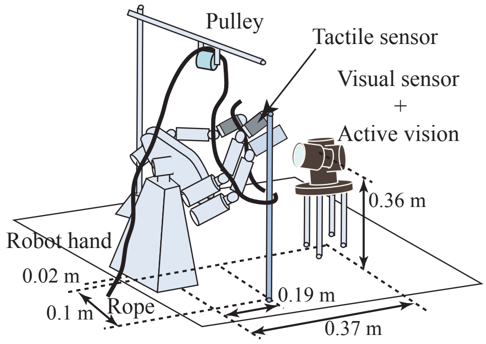

Fig. 21. Overall system for half hitch production.

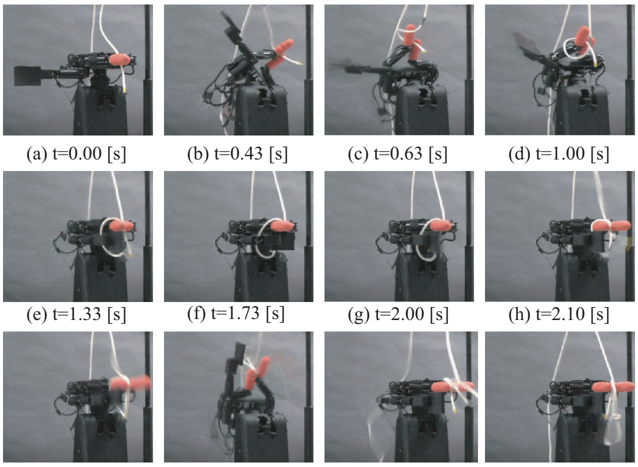

(a) t=0.00 [s] (b) t=0.43 [s] (c) t=0.63 [s] (d) t=1.00 [s]
(e) t=1.33 [s] (f) t=1.73 [s] (g) t=2.00 [s] (h) t=2.10 [s]
(i) t=2.27 [s] (j) t=2.37 [s] (k) t=2.67 [s] (l) t=3.13 [s]

Fig. 20. Continuous photographs of overhand knot.

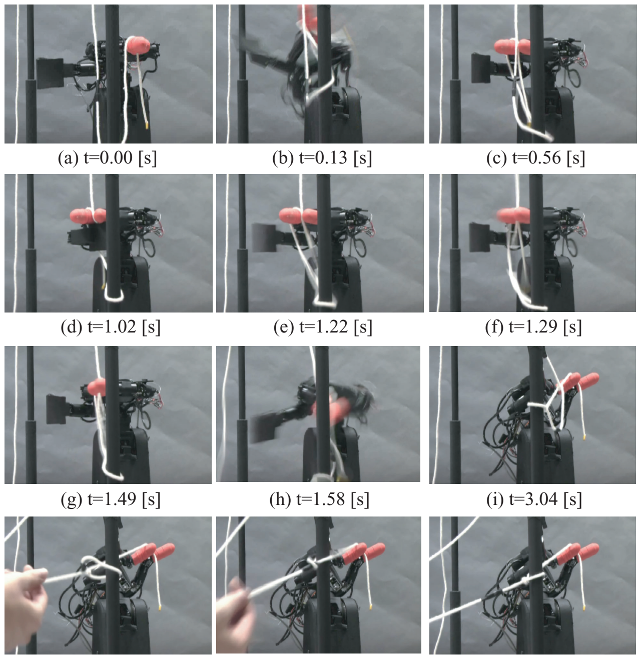

(a) t=0.00 [s] (b) t=0.13 [s] (c) t=0.56 [s]
(d) t=1.02 [s] (e) t=1.22 [s] (f) t=1.29 [s]
(g) t=1.49 [s] (h) t=1.58 [s] (i) t=3.04 [s]
(j) t=4.98 [s] (k) t=5.58 [s] (l) t=6.50 [s]

Fig. 22. Continuous photographs of half hitch production.

7. Conclusion

Our goal was to achieve knotting of a flexible rope as an example of dexterous manipulation of a linear flexible object.

First, we analyzed the knotting motion of a human hand to identify the necessary knotting skills. Then, we proposed a knot description methodology and a method of obtaining the production process of a knot based on skill synthesis.

Second, we suggested a knotting strategy that does not depend on the flexible characteristics of the rope. A real-time tactile and visual sensory feedback control method was proposed to improve the success rate and robustness for various ropes.

Last, we demonstrated experimental results achieved by a high-speed multifingered hand system.

References

[1] H. Inoue and M. Inaba, Hand-eye Coordination in Rope Handling, *Robotics Research: The First International Symposium, MIT Press*, pp. 163–174, 1984.

[2] T. Matsuno, T. Fukuda, and F. Arai, Flexible Rope Manipulation by Dual Manipulator System Using Vision Sensor, *Proc. IEEE/ASME Int. Conf. on Advanced Intelligent Mechatronics*, pp. 677–682, 2001.

[3] T. Morita, J. Takamatsu, K. Ogawara, H. Kimura, K. Ikeuchi, Knot Planning from Observation, *Proc. IEEE Int. Conf. on Robotics and Automation*, pp. 3887–3892, 2003.

[4] H. Wakamatsu, E. Arai, and S. Hirai, Knotting/Unknotting Manipulation of Deformable Linear Objects, *Int. J. Robot. Res.*, Vol. 25, No. 4, pp. 371–395, 2006.

[5] Y. Yamakawa, A. Namiki, M. Ishikawa and M. Shimojo, Knotting Manipulation of a Flexible Rope with a High-speed Multifingered Hand System based on Skill Synthesis. *Proc. Int. Conf. Intelligent Robots and Systems*, pp. 2691–2696, 2008.

[6] A. Namiki, Y. Imai, M. Ishikawa, and M. Kaneko, Development of a High-speed Multifingered Hand System and Its Application to Catching, *Proc. Int. Conf. Intelligent Robots and Systems*, pp. 2666–2671, 2003.

[7] M. Ishikawa and M. Shimojo, A Method for Measuring the Center Position of a Two Dimensional Distributed Load Using Pressure-Conductive Rubber, *Trans. The Society of Instrument and Control Engineers*, Vol. 18, No. 7, pp. 730–735, 1982 (in Japanese).

[8] Y. Nakabo, M. Ishikawa, H. Toyoda, and S. Mizuno, 1ms column parallel vision system and its application of high speed target tracking, *Proc. of IEEE Int. Conf. on Robot. and Automat.*, pp. 650–655, 2000

[9] Y. Yamakawa, A. Namiki, M. Ishikawa and M. Shimojo, One-handed Knotting of a Flexible Rope with a High-speed Multifingered Hand having Tactile Sensors. *Proc. Int. Conf. Intelligent Robots and Systems*, pp. 703–708, 2007.

[10] http://www.k2.t.u-tokyo.ac.jp/fusion/Knotting/